G condition in the F2 region peak electron density: a statistical study

V. V. Lobzin, A. V. Pavlov

Annales Geophysicae (2002) 20: 523–537 © European Geophysical Society 2002

Annales Geophysicae

G condition in the F2 region peak electron density: a statistical study

V. V. Lobzin and A. V. Pavlov

Institute of Terrestrial Magnetism, Ionosphere, and Radio-Wave Propagation, Russian Academy of Sciences (IZMIRAN), Troitsk, Moscow Region, 142190, Russia

Received: 18 January 2001 – Revised: 20 August 2001 – Accepted: 27 September 2001

Abstract. We present a study of statistical relationships between the G condition, F1-layer and NmF2 negative disturbance occurrence probabilities and geomagnetic and solar activity indices K_p and F10.7, season, and geomagnetic latitude, using experimental data acquired by the Ionospheric Digital Database of the National Geophysical Data Center, Boulder, Colorado from 1957 to 1990. It is shown that the dependence of the G condition occurrence probability, Ψ_G, on K_p is mainly determined by processes that control the behaviour of the F2 layer with K_p changes. We found that the relationship for log Ψ_G versus K_p is very close to the linear one. The G condition occurrence probability decreases from 0.55% to 0.17% as the value of F10.7 increases from low to middle values, reaches its minimum at the middle solar activity level of F10.7 = 144 – 170, increasing from the minimum value of 0.17% to 0.49% when the F10.7 index increases from the middle solar activity level to F10.7 = 248 – 274. Interhemispheric asymmetry is found for the G condition occurrence probability in the ionosphere, with a stronger enhancement seen in the magnetic latitude range close to the northern magnetic pole and a deep minimum of the G condition occurrence probability in the low magnetic latitude range from $-30°$ to $30°$. The measured magnetic latitude variation of the F1-layer occurrence probability is also asymmetrical relative to the geomagnetic equator. Our results provide additional evidence the F1-layer is more likely to be formed in summer than in winter. The Northern Hemisphere peak F1-layer occurrence probability is found to exceed that in the Southern Hemisphere. The G condition occurrence probability has maximum values of 0.91 and 0.75% in summer, and minimum values of 0.01 and 0.05% in winter for the Northern and Southern Hemisphere, respectively.

Key words. Ionosphere; ion chemistry and composition; ionosphere-atmosphere interactions; ionospheric disturbances

Correspondence to: A. V. Pavlov (pavlov@izmiran.rssi.ru)

1 Introduction

The Ionospheric Digital Database of the National Geophysical Data Center, Boulder, Colorado, provides the routine sounding ground-based station measurements of the critical frequencies and virtual heights of different ionospheric layers extracted from ionograms; in particular, the critical frequencies fof1 and fof2 of the F1 and F2 layers that are analyzed in this study. This Database is formed using the rules of the URSI standard (URSI handbook of ionogram interpretation and reduction, 1978). In addition to numerical values of ionospheric parameters, the qualifying and descriptive letters A–Z are used in this Database. The descriptive letter G means that a measurement is influenced, or impossible, because the ionization density of the layer is too small to enable it to be made accurately; this case is described as a G condition in the F-region of the ionosphere when fof2 ≤ fof1 (URSI handbook of ionogram interpretation and reduction, 1978). If the layer is not seen from ionograms due to other reasons, then other letters are used. For example, the letter *R* is used if the layer is influenced by, or is not seen from ionograms due to, attenuation of radio waves. The aim of this paper is to carry out a statistical study of a G condition using the Digital Database fof2 measurements, i.e. the ground-based ionosonde measurements of the F2-region peak electron densities, NmF2.

The G condition arises in the ionosphere when the critical frequency of the F2-layer drops below that of the F1-layer, i.e. when the peak density, NmF1, of the F1-layer, which is composed mostly of the molecular ions NO^+ and $O_2{}^+$, is larger than that of the F2-layer, which is dominated by O^+ ions (King, 1962). As a result, a very low main peak altitude, hmax, value (below 200 km) is observed in ionograms, so that no information is obtainable above this height from ground-based ionosonde data. As far as the authors know, the first altitude distribution of the electron density with NmF2 ≤ NmF1 (G condition) was deduced by Norton (1969) from ionograms recorded by the Alouette I satellite ionosonde and the St. John's ground-based ionosonde during the severe negative ionospheric storm on 18 April 1985.

The physics of this phenomenon has been studied by

Buonsanto (1990) using ionosonde data from two mid-latitude stations, Boulder and Wallops Island, by Oliver (1990) using Millstone Hill incoherent scatter radar (ISR) data, and by Fukao et al. (1991) using data from the middle and upper atmosphere radar in Japan. Pavlov and Buonsanto (1998), Pavlov (1998), Pavlov et al. (1999), and Schlesier and Buonsanto (1999) studied the G condition formation for quiet and disturbed mid-latitude ionosphere during periods of low, moderate, and high solar activity using the Millstone Hill ISR data. Model results also show that O^+ can become a minor ion in the F-region creating G condition during disturbed conditions at high latitudes (Banks et al., 1974; Schunk et al., 1975); observations at EISCAT confirm this conclusion (e.g., Häggström and Collis, 1990). These papers provide evidence that changes in [O], [N_2], [O_2] and the plasma drift velocity, the effect of the perpendicular (with respect to the geomagnetic field) component of the electric field on the electron density (through changes in the rate coefficients of chemical reactions of ions), and the effects of vibrationally excited N_2 and O_2 on the electron density are important factors that control the G condition formation in the ionosphere. This means that the probability of G condition occurrence depends on the daily solar activity index, F10.7, the 3-h geomagnetic index, K_p, the number, n_d, of a given day in a year and the geomagnetic latitude, φ. As far as the authors know, although the anomalous structure of the ionosphere has been observed on ionograms and by ISR for many years, there are no published studies of the statistical relationship of G condition occurrences with K_p, F10.7, φ and n_d. The main purpose of this work is to study, for the first time, these statistical relationships and to evaluate the probability of the G condition occurrence.

During NmF2 disturbances, believed to be caused by geomagnetic storms and substorms, NmF2 decreases (NmF2 negative disturbances) lead to increases in the G condition occurrence probability if the F1-layer exists. On the other hand, the G condition cannot exist in the ionosphere if there is no the F1-layer. In our analysis we study a possible relationship of the probability of the G condition occurrence with the probabilities of the F1-layer occurrence and the NmF2 negative disturbance occurrence.

2 The formation of the F1- and F2-layers in the ionosphere

The F-region is located in the altitude range above 140–160 km. Within the F-region are the F1 and F2-layers with peak altitudes hmF1$<$ 190–200 km and hmF2$>$ 200–210 km. The major F1- and F2-layer ions are $O^+(^4S)$, $O_2{}^+$, and NO^+ ions. The F-region behaviour is controlled by physical processes described in many review articles and books on the formation of the ionosphere (e.g. Ratcliffe, 1972; Rishbeth and Garriot, 1969; Brunelli and Namgaladze, 1988; Rees, 1989; Fejer, 1997). The present section is not intended to be a comprehensive review. Its purpose is to point out the main physical processes that form the F1- and F2-layers in the ionosphere by a balance between production, chemical loss, and transport of electrons and ions.

2.1 Ionization of neutral species by solar radiation and by auroral electrons

Solar extreme ultraviolet (EUV) radiation photoionizes the main neutral species N_2, O_2 and O in the thermosphere, producing electrons and $N_2{}^+$, $O_2{}^+$ and O^+ ions. Ionization of N_2, O_2, and O by photoelectrons produces little extra $N_2{}^+$, $O_2{}^+$ and O^+ ions. At high latitudes, there is a source of ionization in the auroral oval which exists in both the Northern and Southern hemispheres above about 60° geomagnetic latitude. Auroral electrons come from the magnetosphere and spiral down the magnetic field lines of the Earth, producing $N_2{}^+$, $O_2{}^+$ and O^+ ions by ionization of the main neutral species N_2, O_2 and O. Auroral charged particle precipitation is characterized by long-term unpredictability and highly variable strength and spatial inhomogeneity (Rees, 1989).

At the F2 peak altitude, the atomic species dominate, with $O^+(^4S)$ and O being the major ion and neutral species, respectively. Following Richards et al. (1994), we conclude that about 60% of the oxygen ions are created in electronically excited states ^2D, ^2P, ^4P and $^2P^*$ during atomic oxygen photoionization. As the radiation flux penetrates into the atmosphere it is attenuated owing to absorption. The results of many theoretical studies (see Ratcliffe, 1972; Rishbeth and Garriot, 1969; Brunelli and Namgaladze, 1988, and references therein) provide sufficient evidence to neglect the effects of this absorption on production rates of oxygen ions at the daytime F2 peak altitudes. Therefore, the production rate, $P(^4S)$ of unexcited oxygen ions and the production rates, $P(^2D)$, $P(^2P)$, $P(^4P)$, and $P(^2P^*)$ of excited oxygen ions by photoionization and by photoelectrons are proportional to [O] and the $P(^4S)$/[O], $P(^2D)$/[O], $P(^2P)$/[O] and $P(^2P^*)$/[O] ratios do not depend on neutral number densities during daytime conditions.

The excited oxygen ions are converted to unexcited $O^+(^4S)$ ions and $N_2{}^+$ and $O_2{}^+$ ions by chemical reactions that are included in current models of the ionosphere and plasmasphere (e.g. Torr et al., 1990; Pavlov, 1997). As a result, the total production rate, $P(O^+)$, of $O^+(^4S)$ ions (that is the sum of $P(^4S)$ and the production rate of $O^+(^4S)$ ions from excited oxygen ions by chemical reactions) is proportional to [O] and there is some dependence of the $P(O^+)$/[O] ratio on [O], [N_2] and [O_2] at the daytime F2 peak altitudes (for more details see Eq. (A3) of Pavlov and Buonsanto, 1997). It should be noted that near sunrise and sunset the optical depths become large for the important radiations in the F2-layer and the production rate of O^+ ions by photoionization depends strongly on the (O)/[N_2] ratio (Rishbeth and Garriot, 1969).

2.2 Loss rate of $O^+(^4S)$ ions

Unexcited $O^+(^4S)$ ions that predominate at F2 region altitudes are lost in the reactions of $O^+(^4S)$ with unex-

cited N_2(v=0) and O_2(v=0) and vibrationally excited N_2(v) and O_2(v) molecules at vibrational levels, v>0, converting $O^+(^4S)$ ions to NO^+ and $O_2{}^+$ ions by

$$O^+(^4S) + N_2(v) \rightarrow NO^+ + N, \quad (1)$$

$$O^+(^4S) + O_2(v) \rightarrow O_2{}^+ + O \quad (2)$$

with the loss rate

$$L = \beta[N_2] + \gamma(O_2], \quad (3)$$

where v = 0,1,... is the number of the vibrational level of N_2 or O_2. The effective rate coefficients of reactions (1) and (2) are determined as (Pavlov, 1998)

$$\beta = \sum_{v=0}^{\infty}[N_2(v)]\beta_v/[N_2], \gamma = \sum_{v=0}^{\infty}[O_2(v)]\gamma_v/[O_2], \quad (4)$$

where β_v is the recombination rate coefficient of $O^+(^4S)$ ions with N_2(v), γ_v is the recombination rate coefficient of $O^+(^4S)$ ions with O_2(v) and the total N_2 and O_2 number densities are determined as

$$[N_2] = \sum_{v=0}^{\infty}[N_2(v)] \text{ and}$$

$$[O_2] = \sum_{v=0}^{\infty}[O_2(v)], [N_2(v)] \text{ and } [O_2(v)]$$

are the number densities of N_2 and O_2 at the v-th vibrational level.

The model of the Boltzmann distribution determines the number densities of vibrationally excited N_2(v) and O_2(v) as

$$[N_2(v)] = [N_2(0)]\exp(-v\,E_1\,T_{N2v}{}^{-1}),$$
$$[O_2(v)] = [O_2(0)]\exp(-v\,E_1{}'\,T_{O2v}{}^{-1}), \quad (5)$$

where E_1 = 3353 K is the energy of the first level of N_2 given by Radzig and Smirnov (1985), $E_1{}'$ = 2239 K is the energy of the first level of O_2 given by Radzig and Smirnov (1985).

It follows from Eq. (5) that

$$[N_2] = [N_2(0)]\{1 - \exp(-E_1\,T_{N2v}{}^{-1})\}^{-1},$$
$$[O_2] = [O_2(0)]\{1 - \exp(-E_1{}'\,T_{O2v}{}^{-1})\}^{-1}. \quad (6)$$

Schmeltekopf et al. (1968) measured the dependence of β on the N_2 vibrational temperature, T_{N2v} , over the vibrational temperature range 300–6000 K when the neutral and ion temperatures, T_n and T_i, are fixed at 300 K. The values of β_v for the vibrational levels v = 1 – 11 were extracted by Schmeltekopf et al. (1968) from the measured dependence of β on T_{N2v}. As a result, the β_v/β_0 ratios for $T_n = T_i$ = 300 K can be determined for the vibrational levels v = 1–5 that are usually included in the model calculations (Pavlov, 1998; Pavlov et al., 1999) as

$$\beta_1/\beta_0 = 1, \beta_2/\beta_0 = 38, \beta_3/\beta_0 = 85,$$
$$\beta_4/\beta_0 = 220, \beta_5/\beta_0 = 270. \quad (7)$$

The measurements of β were presented by Hierl et al. (1997) over the temperature range 300–1600 K for $T_n = T_i = T_{N2v}$. The fundamental results of Hierl et al. (1997) confirm the observations of Schmeltekopf et al. (1968), and show for the first time that the translation temperature dependencies of β_v are similar to β_0. This means that the β_v/β_0 ratios given by Eq. (7) are valid for $T_n = T_i$ = 300–1600 K and that these β_v/β_0 ratios can be used to model the F-region of the ionosphere.

Hierl et al. (1997) determined the dependence of γ on the O_2 vibrational temperature, T_{O2v}, over the temperature range 300–1800 for $T_{O2v} = T_n = T_i$. The flowing afterglow measurements of γ given by Hierl et al. (1997) were used by Hierl et al. (1997) and Pavlov (1998) to invert the data to find the rate coefficient γ_v, for the various vibrational levels of O_2(v>0) as

$$\gamma_1/\gamma_0 = 1, \gamma_2/\gamma_0 = 5, \gamma_3/\gamma_0 = 50,$$
$$\gamma_4/\gamma_0 = 50, \gamma_5/\gamma_0 = 50. \quad (8)$$

The thermal rate coefficients β_0 and γ_0 depend on T_n, T_i, and a relative drift velocity, V_d, between ions and molecules (which is a function of the perpendicular component, $E_\perp$, of the electric field with respect to the geomagnetic field) only by means of an effective temperature (St.-Maurice and Torr, 1978)

$$T_{eff} = (m_i T_n + m_n T_i)(m_i + m_n)^{-1}$$
$$+ m_i\,m_n\,V_d{}^2\,(m_i + m_n)^{-1}\,(3k)^{-1}, \quad (9)$$

where k is the Boltzmann constant, m_i and m_n denote the masses of the ion and neutral reactants, respectively.

As a result, we conclude that the loss rate of $O^+(^4S)$ ions is a function of $[N_2]$, $[O_2]$, T_n, T_i, $E_\perp$, T_{N2v} and T_{O2v}.

The excitation of N_2 and O_2 by thermal electrons provides the main contribution to the values of N_2 and O_2 vibrational excitations if the electron temperature, T_e, is higher than about 1600–1800 K at F-region altitudes; the values of T_{N2v} and T_{O2v} are close to T_n for T_e <1600–1800 K and the values of $T_{N2V} - T_n$ and $T_{O2V} - T_n$ increase with increasing the electron temperature (Pavlov, 1988, 1994, 1997, 1998; Pavlov and Namgaladze, 1988; Pavlov and Buonsanto, 1997; Pavlov and Oyama, 2000; Pavlov et al., 2000, 2001). This means that the loss rate of $O^+(^4S)$ ions is a function of (N_2), (O_2), T_n, T_i, $E_\perp$ and T_e. Our calculations show that an increase in the effective temperature results in an increase of β for T_{eff} > 920 K and in an increase of γ for T_{eff} > 850 K if $T_{eff} = T_{N2V} = T_{O2V}$. The variation of β is less than 20% in the effective temperature range of 620 K –1170 K and the variation of γ is less than 20% in the effective temperature range of 550 K –1240 K if $T_{eff} = T_{N2V} = T_{O2V}$.

2.3 Transport of electrons and ions

In the F2-layer, both neutral wind induced and field-aligned diffusion of $O^+(^4S)$ ions and electrons are important in addition to chemical reactions. Electric fields of magnetospheric origin are mapped along geomagnetic field lines to the high

latitude ionosphere. These electric fields are perpendicular to the geomagnetic field and cause the high latitude ionosphere to move approximately horizontally across the polar region at F-region altitudes. The geomagnetic field lines at high latitudes are not completely vertical and the electric field-induced plasma motion has a vertical component which has an effect on both $NmF2$ and $hmF2$. There are also electric fields associated with neutral wind induced ionospheric currents. In the daytime equatorial F2-layer, electrons and ions are lifted to great heights by the eastward electric fields (the electromagnetic drift of plasma), that exist in low latitudes by day, and then diffuse downward along field lines. The result of this plasma transport is that the daytime latitude distribution of $NmF2$ has a minimum value (the equatorial trough in $NmF2$) in the vicinity of the geomagnetic equator and two peaks on each side of the magnetic equator. At the geomagnetic equator, $hmF2$ is largely controlled by the electromagnetic drift which is directed upward by day and downward at night.

2.4 Formation of the ionospheric F2-layer

The characteristic time for the decay of $[O^+(^4S)]$ by the chemical reactions (1) and (2) is obtained as $\tau_c = L^{-1}$. The characteristic diffusion time of $O^+(^4S)$ ions can be determined at middle and high latitudes as $\tau_D = H_p{}^2\, D_a{}^{-1}$, where $D_a = \sin^2 I\,(T_e + T_i)\,k\,(m_i\,\nu_i)^{-1}$ is the ambipolar diffusion coefficient, I is the magnetic dip angle, m_i is the ion mass, ν_i is the collisional frequency of $O^+(^4S)$ ions with oxygen atoms, $H_p = k\,(T_e + T_i)\,(m_i\,g)^{-1}$ is the characteristic scale length and g is the acceleration due to gravity.

In the F1-layer, the value of τ_c is much less than the value of τ_D. Therefore, the photochemistry dominates in the F1-layer and the steady state daytime F1-layer number density of $O^+(^4S)$ ions is directly proportional to the [O]/L ratio, i.e. the value of $[O^+(^4S)]$ increases with altitude. The value of D_a increases exponentially with altitude owing to its dependence on [O] ($D_a \sim [O]^{-1}$) and, hence at high altitudes, diffusion dominates. As a result, if the plasma drift effect on hmF2 is unimportant, the height of the middle and high latitude F2 peak is located approximately at the altitude level where the characteristic times for diffusion and chemistry are equal (Strobel and McElroy, 1970; Ratcliffe, 1972; Rishbeth and Garriot, 1969; Brunelli and Namgaladze, 1988). The F2 peak altitude is lowered by the action of a wind-induced downward plasma drift, due to a poleward wind, and a wind-induced upward plasma drift, caused by an equatorward wind, acts to raise the F2 peak altitude (Strobel and McElroy, 1970; Ratcliffe, 1972; Rishbeth and Garriot, 1969; Brunelli and Namgaladze, 1988).

In order to find the analytical solution of the steady state continuity equation for O^+ ions during quiet days for mid-latitudes, Badin and Deminov (1982) and Badin (1989) assumed that the optical depth of the atmosphere goes to zero, the drift velocity of the plasma in the vertical direction does not depend on the altitude, $T_i \approx$ const, $T_n \approx$ const, and $T_e \approx$ const. As a consequence of this analytical approach, $NmF2$ is directly proportional to $[O]^{4/3}\,L^{-2/3}$ (Badin, 1989; Pavlov and Buonsanto, 1997).

The relationship between $NmF2$ and the [O]/L ratio is complicated by effects of plasma drifts due to electric fields and neutral winds (see Sect. 2.3) on $NmF2$ and by some dependence of the $P(O^+)/[O]$ ratio on [O], $[N_2]$ and $[O_2]$ (see Sect. 2.1). Nevertheless, the $[O]/[N_2]$ ratio measured by satellites (e.g. by the ESRO 4 satellite) and the F2 peak density measured by ionosonde stations are similar (Prolss, 1980, 1995) and it is usually supposed that the value of $NmF2$ is approximately directly proportional to the [O]/L ratio at $hmF2$ during daytime conditions (Rishbeth and Garriot, 1969; Brunelli and Namgaladze, 1988; Rishbeth and Muller-Wodarg, 1999; Rishbeth et al., 2000). Therefore, this assumption is used in our study in discussions of $NmF2$ variation sources.

2.5 Formation of the ionospheric F1-layer

The role of the ion transport is less than the role of chemical reactions of ions with electrons and neutral components of the upper atmosphere at the F1-layer altitudes, and production and loss rates of electron and ions determine the F1-layer formation.

As is well known, the major molecular ions are $O_2{}^+$ and NO^+ ions in the F-region of the ionosphere. The chemistry of NO^+ ions in the F-region of the ionosphere is comparatively simple, with the NO^+ production via reactions of $O^+(^4S)$ ions with $N_2(v = 0-5)$ given by Eq. (1), $O_2{}^+$ ions with NO and N and $N_2{}^+$ ions with O, and loss through dissociative recombination (for more details see Rishbeth and Garriot, 1969; Brunelli and Namgaladze, 1988; Rees, 1989; Torr et al. 1990; Pavlov, 1997). The O_2 photoionization, the O_2 ionization by photoelectrons and auroral electrons, the chemical reactions of $O^+(^4S)$ ions with unexcited and vibrationally excited O_2 is given by Eq. (2), and $N_2{}^+$ with O_2 are the sources of $O_2{}^+$ ions in the F-region of the ionosphere while the sinks of $O_2{}^+$ ions are dissociative recombination of $O_2{}^+$ and the chemical reactions of $O_2{}^+$ with N and $O_2{}^+$ with NO (for more details see Rishbeth and Garriot, 1969; Brunelli and Namgaladze, 1988; Rees, 1989; Torr et al., 1990; Pavlov, 1997).

To study the formation of the F1-layer, Ratcliffe (1972) assumed that the main source of NO^+ ions is the chemical reaction of O^+ with N_2 and that there are only NO^+ and O^+ ions. Ratcliffe (1972) found that the peak of the F1-layer exists in the ionosphere if the peak altitude, h_0, of the total production rate of thermal electrons is less than the altitude, h_t , that is determined from the condition of $\beta\,[N_2] = \alpha[e]$, where α is the rate coefficient of the dissociative recombination of NO^+ ions. Ratcliffe (1972) concluded that the value of $h_t - h_0$ is decreased with the solar activity level increase and the value of $h_t - h_0$ has a maximum value close to midday. As a result, the F1 peak is more clearly in evidence at solar minimum than at solar maximum and the F1 peak is more commonly formed near midday and in summer (Ratcliffe, 1972).

3 Data and method of data analysis

Ionograms produced by ionosondes are records that show variations of virtual height of radio wave reflection from the ionosphere as a function of the radio frequency, h′(f), within the frequency band range 1 MHz–20 MHz that is normally used (URSI handbook of ionogram interpretation and reduction, 1978). The radio wave that is reflected from the ionosphere level of ionization is split into two waves of different polarization by the Earth's magnetic field thereby leading to two sorts of observed h′(f) curves. These waves are called the ordinary wave (o-mode) and the extraordinary wave (x-mode). There are also z-mode traces on some ionograms, generated by radio waves which have been propagated along the magnetic field lines. The mode traces can be identified by the frequency separation and by other indications presented in URSI handbook of ionogram interpretation and reduction (1978). A simple approach is used to find peak electron densities of the ionosphere from observations of h′(f) curves, i.e. when the level of the peak electron density in the layer is reached, the value of h′(f) becomes effectively infinite

$$\left(\frac{\mathrm{df}}{\mathrm{dh}'} \to 0\right).$$

The frequency at which this occurs is determined as the critical frequency of the ionospheric layer. The values of $NmF2$ and $NmF1$ are related to the critical frequencies $foF2$ and $foF1$ extracted from the h′(f) curve of the ordinary wave as $NmF2 = 1.24 \cdot 10^{10}\ foF2^2$ and $NmF1 = 1.24 \cdot 10^{10}\ foF1^2$, where the unit of $NmF2$ and $NmF1$ is m^{-3} and the unit of $foF2$ and $foF1$ is MHz (URSI handbook of ionogram interpretation and reduction, 1978).

Our analysis is based on 34 years of hourly $foF2$ and $foF1$ data from 1957 to 1990 from stations on the Ionospheric Digital Database of the National Geophysical Data Center, Boulder, Colorado. The total probabilities of the G condition and F1-layer occurrences can be determined as the ratio of total G condition observations to the total number of studied observations and as the ratio of total F1-layer observations to the total number of observations, respectively. We study the dependence of the probabilities of G condition and F1-layer occurrences on F10.7, K_p, $\mathrm{n_d}$ and φ. A sum, $\mathrm{S_G}$, of G condition observations and a sum, $\mathrm{S_{F1}}$, of F1-layer observations over 3 parameters from these 4 parameters are functions of a fourth parameter, X. The G condition probability function, $\Psi_{\mathrm{G}}(\mathrm{X})$, of this fourth parameter has been introduced as a ratio of $\mathrm{S_G}$ to the total number of studied observations, and the F1-layer probability function, $\Psi_{\mathrm{F1}}(\mathrm{X})$, of the same parameter has been introduced as a ratio of $\mathrm{S_{F1}}$ to the total number of studied observations. To investigate $\Psi_{\mathrm{G}}(\mathrm{X})$ and $\Psi_{\mathrm{F1}}(\mathrm{X})$ dependencies, we split the range of X into twelve intervals of the same length and calculate the $\Psi_{\mathrm{G}}(\mathrm{X})$ and $\Psi_{\mathrm{F1}}(\mathrm{X})$ variations. The following investigation seeks to find these probability function variations.

The electron density can either decrease or increase during geomagnetically disturbed conditions, and these changes in the electron density are denoted as negative and positive ionospheric disturbances, respectively. To test the effects of geomagnetic activity, we use two different K_p labels: "disturbed", for which we take $K_p > 3$ and use the peak density, $NmF2(\mathrm{d})$ and critical frequency, $foF2(\mathrm{d})$, of the F2-layer observed during the time periods with $K_p > 3$, and "quiet", for which we take $K_p \leq 3$. The determination of the quiet peak density, $NmF2(\mathrm{q})$ and critical frequency, $foF2(\mathrm{q})$, of the F2-layer, is crucial for studies of negative and positive ionospheric disturbances. When the thermosphere is disturbed, the time it takes to relax back to its initial state and this thermosphere relaxation determines the time for the disturbed ionosphere to relax back to the quiet state. This means that not every $foF2$ observed during the day with $K_p \leq 3$ can be considered as $foF2(\mathrm{q})$. The characteristic time of the neutral composition recovery after a storm impulse event ranges from 7 h to 12 h on average (Hedin, 1987) while it is may need up to days for all altitudes down to 120 km in the atmosphere to recover completely back to the undisturbed state of the atmosphere (Richmond and Lu, 2000). Therefore, we determine the quiet reference day with $foF2(\mathrm{q})$ by the choice of the quiet day with $K_p \leq 3$ from 00:00 UT to 24:00 UT if the previous day was the day with $K_p \leq 3$ from 00:00 UT to 24:00 UT. Furthermore, we use only quiet days with uninterrupted $foF2$ measurements from 00:00 UT to 24:00 UT; the comparison between $foF2(\mathrm{d})$ and $foF2(\mathrm{q})$ measured at the chosen station is carried out if the time difference between $foF2(\mathrm{d})$ and $foF2(\mathrm{q})$ measurements is less than or equal to 30 days. We use the nearest quiet day to the studied disturbed time period, and determine the relative deviation, δ, of $foF2$ observed at the given station from $foF2(\mathrm{q})$ as

$$\begin{aligned}\delta &= \mathrm{fof2(d)/fof2(q)} - 1 \\ &= \{\mathrm{NmF2(d)/NmF2(q)}\}^{1/2} - 1. \end{aligned} \tag{10}$$

Negative and positive values of δ correspond to negative and positive disturbances in $NmF2$, respectively. We study the dependence of the probabilities of negative and positive disturbance occurrences in $NmF2$ on K_p, $\mathrm{n_d}$, φ and F10.7. The sum, $\mathrm{S}_{\delta<0}$, of negative disturbance observations and the sum, $\mathrm{S}_{\delta>0}$, of positive disturbance observations, over 3 parameters from these 4 parameters, are functions of a fourth parameter, X. The negative disturbance probability function, $\Psi_{\delta<0}(\mathrm{X})$, of this fourth parameter has been introduced as a ratio of $\mathrm{S}_{\delta<0}$ to the total number of studied disturbed observations, and the positive disturbance probability function, $\Psi_{\delta>0}(\mathrm{X})$, of the same parameter has been introduced as a ratio of $\mathrm{S}_{\delta>0}$ to a total number of studied disturbed observations. To investigate $\Psi_{\delta<0}(\mathrm{X})$ and $\Psi_{\delta>0}(\mathrm{X})$ dependencies, we split the range of X into twelve intervals of the same length and calculate the $\Psi_{\delta<0}(\mathrm{X})$ and $\Psi_{\delta>0}(\mathrm{X})$ variations.

The $NmF2$ decrease leads to the increase in the G condition occurrence probability. As a result, it is possible that only strong negative $NmF2$ disturbances can be important to explain the G condition occurrence trends. Therefore, it is necessary to consider the probability, $\Psi_{\delta\leq\delta 0}(\mathrm{X})$, of negative disturbance occurrences in $NmF2$ for $\delta \leq \delta 0 < 0$. We calculate a sum, $\mathrm{S}_{\delta\leq\delta 0}$, of negative disturbance observations

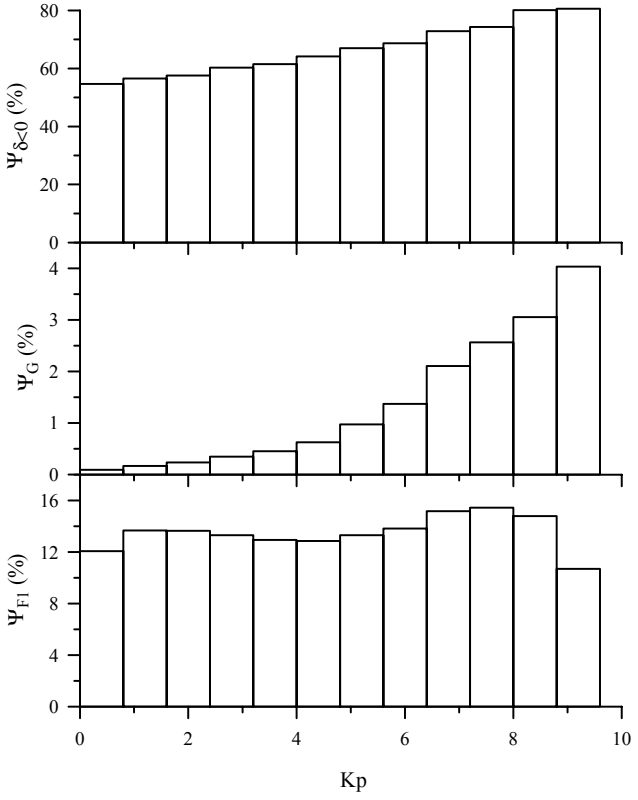

Fig. 1. The dependence of the F1-layer (bottom panel), G condition (middle panel) and NmF2 negative disturbance (top panel) probability functions on the 3-h geomagnetic activity index K_p.

over 3 parameters from the next parameters: K_p, n_d, φ and F10.7. The value of $S_{\delta\le\delta 0}$ is a function of a fourth parameter, X, and $\Psi_{\delta\le\delta 0}(X) = S_{\delta\le\delta 0}(X) / \{S_{\delta<0}(X) + S_{\delta>0}(X)\}$. The calculations of $\Psi_{\delta\le\delta 0}(X)$ were carried out for $\delta 0 = -0.1$, -0.3 and -0.5; these values of $\delta 0$ correspond to 0.81, 0.49 and 0.25 in the NmF2(d) / NmF2(q) ratio, respectively. We give negative fof2 disturbances the labels "weak", "normal", "strong" and "very strong" for $-0.1<\delta<0$, $-0.3<\delta\le-0.1$, $-0.5<\delta\le -0.3$, $\delta\le-0.5$, respectively, and confine our attention to relationships between them and G condition occurrences.

Our analysis is carried out by sorting the data versus one independent parameter (K_p, n_d, φ and F10.7), i.e. single-parameter statistics is used. This approach can be considered as the first step in our studies of the NmF2 negative disturbance, G condition and F1-layer occurrence probabilities; we plan to use multiple-parameter statistics in our future studies of these probabilities.

4 Results and discussion

The total number of hourly measurements studied is 20 532 879 which include 69 443 G condition occurrences and 2 711 074 F1-layer occurrences. Thus, we found that the total probabilities of the G condition and F1-layer occurrences for the time period from 1957 to 1990 to be 0.34% and 13.20%, respectively. Our calculations of $\Psi_{\delta<0}(X)$, $\Psi_{\delta>0}(X)$ and $\Psi_{\delta\le\delta 0}(X)$ (i.e. NmF2 disturbance analysis) includes only negative and positive ionospheric disturbances that have reference quiet days (see Sect. 3). A part of the hourly fof2 disturbance measurements has no reference quiet days in agreement with the quiet day definition accepted in our paper, and these hourly fof2 measurements are not analyzed. The total number of the analyzed hourly fof2 disturbance measurements that have quiet days includes 60% of fof2 measurements with $\delta < 0$ and 40% of fof2 measurements with $\delta \ge 0$ for the time period from 1957 to 1990. The analyzed hourly fof2 measurements with $\delta < 0$ includes 47% of weak hourly negative fof2 disturbances ($-0.1 < \delta < 0$ or $0.81 < Nm$F2(d) / NmF2(q) < 1), 43% of normal hourly negative fof2 disturbances ($-0.3 < \delta \le -0.1$ or $0.49 < Nm$F2(d) / NmF2(q) ≤ 0.81), 9% of strong hourly negative fof2 disturbances ($-0.5 < \delta \le -0.3$ or $0.25 < Nm$F2(d) / NmF2(q) ≤ 0.49) and 1% of very strong hourly negative fof2 disturbances ($\delta \le -0.5$ or NmF2(d) / NmF2(q) ≤ 0.25).

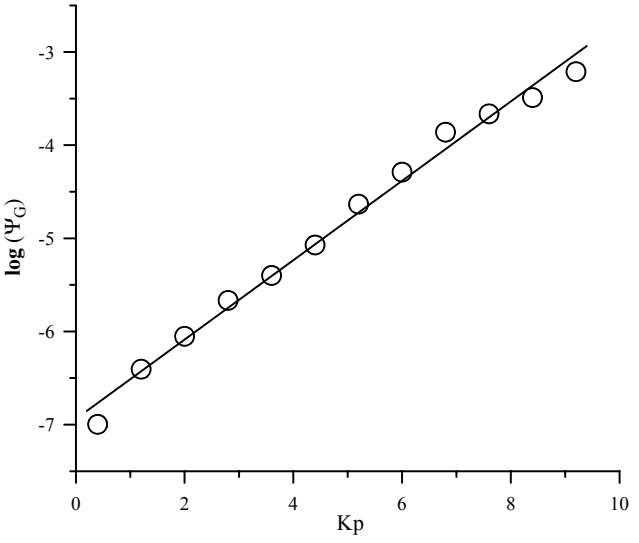

Fig. 2. The statistical relationship (circles) and linear approximation (solid line) for $\log \Psi_G(K_p)$ versus K_p.

4.1 Magnetic activity trends in the F1-layer, G condition and NmF2 negative disturbance occurrence probabilities

Figure 1 shows the probability $\Psi_{F1}(K_p)$ of F1-layer occurrence (bottom panel), the probability $\Psi_G(K_p)$ of the G condition occurrence (middle panel), and the probability $\Psi_{\delta<0}(K_p)$ of the negative disturbance occurrence in NmF2 (top panel) as functions of K_p. Circles displayed in Fig. 2 shows $\log \Psi_G$ versus K_p that is clearly very close to linear. We found that this dependence can be approximated as

$$\log\Psi_G(K_p) = A + B\,K_p \qquad (11)$$

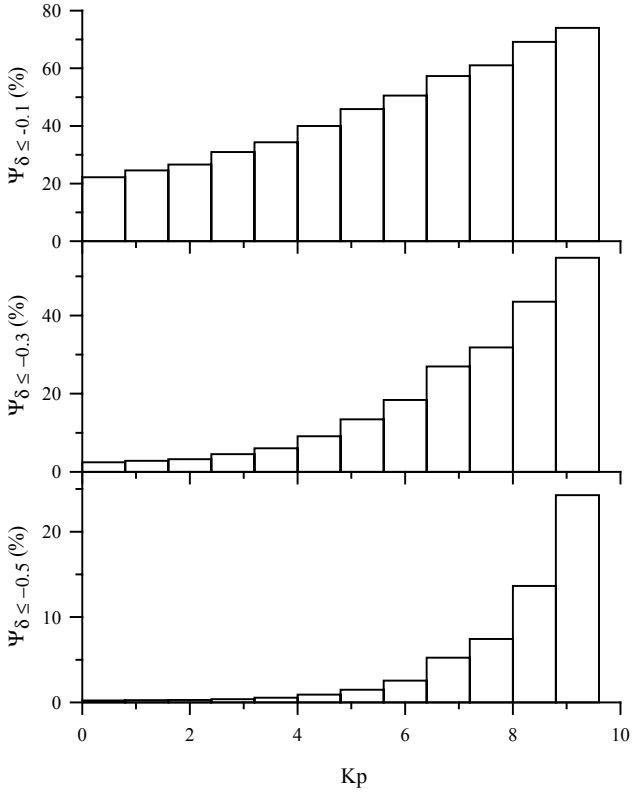

Fig. 3. The dependence of the NmF2 negative disturbance probability functions on the 3-h geomagnetic activity index K_p for the values of the NmF2 negative disturbance amplitude $\delta \leq -0.1$ (top panel), $\delta \leq -0.3$ (middle panel) and $\delta \leq -0.5$ (bottom panel).

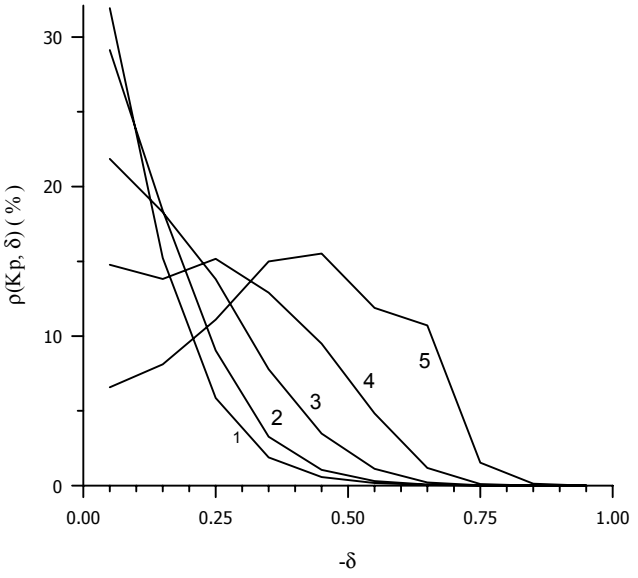

Fig. 4. The dependence of the NmF2 negative disturbance probability density function, $\rho(K_p, \delta)$, on K_p and δ. Lines 1, 2, 3, 4 and 5 show the calculated values of $\rho(K_p, \delta)$ for $K_p = 1$, 3, 5, 7 and 9, respectively.

where the coefficients A = -6.94 ± 0.03, B = 0.426 ± 0.012 are found by the method of least squares. This linear dependence is shown by the solid line in Fig. 2. In contrast to Fig. 1, the values of $\Psi_G(K_p)$ presented by Eq. (11) and Fig. 2 are not multiplied by a factor of 100 (the unit of $\Psi_G(K_p)$ is not percentage).

It can be seen from Fig. 1 that $\Psi_G(K_p)$ and $\Psi_{\delta<0}(K_p)$ reveal the increase with geomagnetic activity, whereas $\Psi_{F1}(K_p)$ does change with the K_p variations that could be responsible for the $\Psi_G(K_p)$ changes. This means that the dependence of the probability of the G condition occurrence on K_p is mainly determined by processes that control the behaviour of the F2-layer with K_p changes and $\Psi_G(K_p)$ has no significant relation to $\Psi_{F1}(K_p)$. This result seems to be quite natural because a G condition in the geomagnetically disturbed ionosphere is associated with a significant negative ionospheric storm in NmF2.

The value of $\Psi_{\delta<0}(K_p)$ includes all negative ionospheric disturbances with $\delta < 0$. Figure 3 shows the probabilities $\Psi_{\delta\leq-0.1}(K_p)$ (top panel), $\Psi_{\delta\leq-0.3}(K_p)$ (middle panel), and $\Psi_{\delta\leq-0.5}(K_p)$ (bottom panel) of the NmF2 negative disturbance occurrence as functions of K_p. We found that the values of $\Psi_{\delta<0}(K_p)$, $\Psi_{\delta\leq-0.1}(K_p)$, $\Psi_{\delta\leq-0.3}(K_p)$, and $\Psi_{\delta\leq-0.5}(K_p)$ have minimum values of 54.9%, 22.3%, 2.5% and 0.2% and maximum values of 80.2%, 70.6%, 52.0% and 24.6%, respectively. We conclude that the ratio of the maximum value of $\Psi_{\delta\leq\delta0}(K_p)$ to the minimum value of $\Psi_{\delta\leq\delta0}(K_p)$ is increased with the increase of the minimum absolute value of the NmF2 negative disturbance amplitude, i.e. the $\Psi_{\delta\leq\delta0}(K_p)$ dependence shows a stronger positive K_p tendency with the increase in $|\delta0|$.

Previous F2-layer negative ionospheric disturbance studies (Mednikova, 1980; Zevakina and Kiseleva, 1985; Wrenn et al., 1987; Brunelli and Namgaladze, 1988), based on limited data sets, show that the value of K_p can be used as a rough indicator of the minimum value of δ and the increase in K_p results in the decrease in this minimum value of δ. To check this hypothesis, we calculate the probability density function, $\rho(K_p, \delta)$, of negative disturbance occurrences in NmF2. The relationship between $\Psi_{\delta<0}(K_p)$ and $\rho(K_p, \delta)$ is

$$\psi_{\delta<0}(K_p) = \int_{-1}^{0} \rho(K_p, \delta) d\delta.$$

To estimate the probability density function, we split the range of δ into ten intervals of the same length.

Lines 1, 2, 3, 4, and 5 of Fig. 4 show the calculated values of $\rho(K_p, \delta)$ for $K_p = 1$, 3, 5, 7 and 9, respectively. It follows from Fig. 4 that there is some small amount of strong NmF2 negative disturbance amplitudes for low values of $K_p = 1$ and 3. This means that these NmF2 negative disturbances are the result of the previous history of geomagnetic activity. We found that there is a difference in the dependence of the probability density function on δ for $K_p \leq 5$ and $K_p \geq 7$. For $K_p \leq 5$, the probability density function is decreased with the decrease in δ in the all of the studied range of δ from

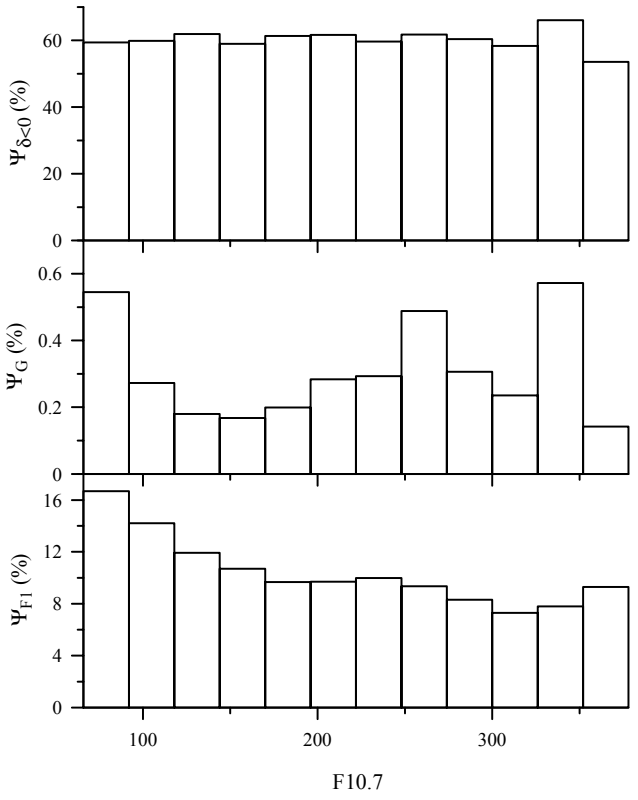

Fig. 5. The dependence of the F1-layer (bottom panel), G condition (middle panel) and NmF2 negative disturbance (top panel) probability functions on the daily solar activity index F10.7.

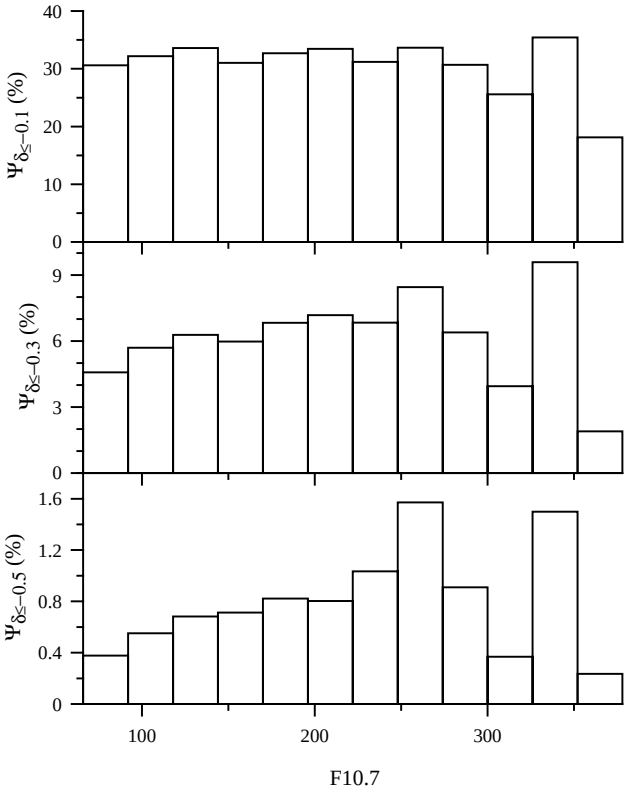

Fig. 6. The dependence of the NmF2 negative storm probability functions on the daily solar activity index F10.7 for the values of the NmF2 negative disturbance amplitude $\delta \leq -0.1$ (top panel), $\delta \leq -0.3$ (middle panel), and $\delta \leq -0.5$ (bottom panel).

0 to 1 while for $K_p = 7$ and 9, the value of $\rho(K_p, \delta)$ is decreased with the decrease in δ only for $\delta < -0.3$ and -0.5, respectively. The maximum values of the probability density function (15.2% and 15.5%) appear for $K_p = 7$ and 9 close to $\delta = -0.25$ and -0.45, respectively. On the other hand, the middle panel of Fig. 1 shows that the increase in K_p leads to the enhancement in the G condition occurrence probability. As a result, the G condition occurrence is associated with large values of $|\delta|$.

The Joule heating of the thermosphere can be viewed as the frictional heating produced in the thermosphere as the rapidly convecting ions collide with neutral molecules; the most part of the Joule heating is deposited in the 115–150 km altitude region, although some extends to higher altitudes (Richmond and Lu, 2000). The geomagnetic storm Joule heating of the thermosphere is considerably more effective than the energy of the auroral electrons in affecting the thermospheric circulation and the increase of the neutral temperature (Richmond and Lu, 2000). Joule heating from the dissipation of ionospheric currents raises the neutral temperature of the upper thermosphere and ion drag drives high-velocity neutral winds during geomagnetic storms at high latitudes (Prolss, 1980, 1995; Fuller-Rowell et al., 1996, 2000). This leads to generation of a disturbed composition zone of the high latitude neutral atmosphere with an increase in the heavier gases and a decrease in the lighter gases, i.e. with an increase in the $[N_2]/[O]$ and $[O_2]/[O]$ ratios. The wind surge propagates from auroral regions to low latitudes in both hemispheres. As a result, thermospheric altitude distribution of neutral species at middle and low latitudes is influenced by a global large scale wind circulation of the neutral atmosphere which is produced by geomagnetic storm energy input at high latitudes (theoretical and observational studies of thermospheric composition responses to the transport of neutral species from auroral regions to middle latitudes during geomagnetic storms are reviewed by Prolss, 1980, 1995). The increase in the $[N_2]/[O]$ ratio maximizes in a region that is roughly located within the auroral oval; this $[N_2]/[O]$ increase intensifies and can expand to middle magnetic latitudes with the K_p increase (Brunelli and Namgaladze, 1988; Prolss, 1980, 1995; Zuzic et al., 1997). The high latitude geomagnetic storm upwelling brings air rich in the heavy species N_2 and O_2 to high altitudes and the geomagnetic storm circulation carries this N_2 and O_2-rich air to mid-latitudes at lower latitudes, the downwelling leads to the opposite effect; air with low values of $[N_2]$ and $[O_2]$ is carried downward, reducing their concentrations at all altitudes (e.g. Fuller-Rowell et al., 1996; Field et al., 1998; Richmond and Lu, 2000). Thus, the values of the $[N_2]/[O]$ and the $[O_2]/[O]$ ratios are enhanced at higher latitudes and depleted at lower latitudes, contributing to high latitude NmF2 decreases and

low latitude $NmF2$ increases during daytime conditions.

The G condition is observed mainly during daytime conditions at middle and high latitudes (Polyakov et al., 1968; Ratcliffe, 1972; see also Sect. 4.3). Until now, the prediction of geomagnetic storm thermospheric variations and perturbations in empirical models have been keyed to geophysical indices like K_p and A_p which are taken to represent the geophysical processes. Thus, the N_2 and O_2 depletion is stronger for high K_p at high and middle latitude; the boundary between N_2 and O_2 enrichment and N_2 and O_2 depletion penetrates to more low latitudes with the increase in K_p.

The MSIS-86 model (Hedin, 1987) simulations show that the neutral temperature is increased with the increase in A_p. This means that the K_p increase can produce the increase of vibrational temperatures of N_2 and O_2 (see Sect. 2.2), leading to some additional increase in the loss rate of the $O^+(^4S)$ ions given by Eq. (3).

As a result, the dependence of $NmF2$ on [O]/L leads to the increases in the $NmF2$ negative disturbance and G condition occurrence probabilities with the K_p increase that are shown in Figs. 1 and 3. However, it remains to be answered why the $\Psi_G(K_p)$ dependence is exponential.

4.2 Dependence of the F1-layer, G condition and $NmF2$ negative disturbance occurrence probabilities on solar activity

The histograms of the dependence of the F1-layer, G condition and $NmF2$ negative disturbance(with $\delta < 0$) percentage occurrences on the daily solar activity index F10.7 are shown in the bottom, middle, and top panels of Fig. 5, respectively.

It can be seen from the bottom panel of Fig. 5 that the value of Ψ_{F1}(F10.7) is decreased with the solar activity index increase. This result agrees with well known conclusions from previous F1-layer studies (for more details see, for example, Polyakov et al., 1968; Ratcliffe, 1972), based on a more limited data set, that the probability to observe the F1-layer is lower at solar maximum then that at solar minimum.

Figure 6 shows the probabilities $\Psi_{\delta\le-0.1}$(F10.7) (top panel), $\Psi_{\delta\le-0.3}$(F10.7) (middle panel) and $\Psi_{\delta\le-0.5}$ (F10.7) (bottom panel) of the $NmF2$ negative disturbance occurrence as functions of F10.7. The top panels of Figs. 5 and 6 show that $\Psi_{\delta<0}$(F10.7) and $\Psi_{\delta\le-0.1}$(F10.7) do not demonstrate the dependence on F10.7. The middle and bottom panels of Fig. 6 show that there is a positive tendency in the $NmF2$ negative disturbance occurrence probability dependencies on F10.7 for strong and very strong negative disturbances with $\delta<-0.3$ and $\delta<-0.5$. The $NmF2$ negative disturbance occurrence probability is increased from 4.6% to 8.5% for $\delta<-0.3$ and from 0.4% to 1.6% for $\delta<-0.5$ with the F10.7 increase from F10.7 = 66–92 to F10.7 = 248–274. Our results show oscillations in the dependence of $\Psi_{\delta\le-0.1}$(F10.7), $\Psi_{\delta\le-0.3}$(F10.7) and $\Psi_{\delta\le-0.5}$(F10.7) on F10.7 above F10.7 = 274.

A prominent feature of the G condition occurrence probability, shown in the middle panel of Fig. 5 is that Ψ_G(F10.7) reaches its minimum at middle solar activity conditions (F10.7 = 144–170). The Ψ_G(F10.7) behaviour contains contributions from two sources, the F1 and F2-layers, and competition of the F10.7 trends in δ and Ψ_{F1}(F10.7) determines Ψ_G(F10.7). The G condition occurrence probability is decreased from 0.55% to 0.17% with the F10.7 increase from F10.7 = 66–92 to F10.7 = 144–170, showing that the main source that contributes to Ψ_G(F10.7) at solar minimum is the dependence of the F1-layer occurrence on F10.7.

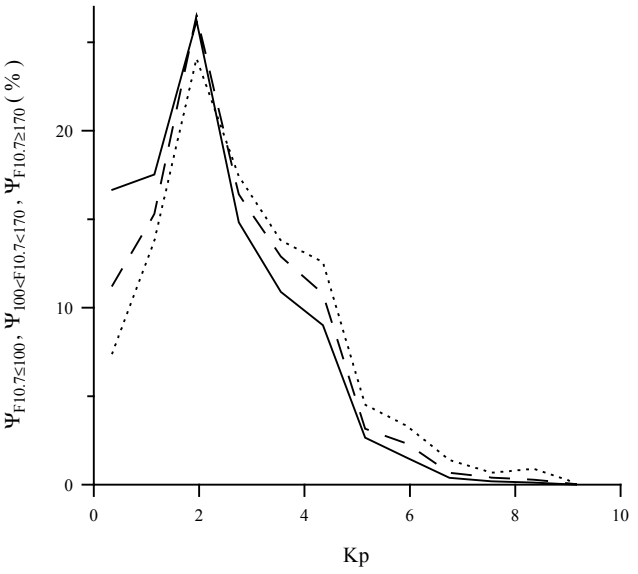

Fig. 7. The conditional probability of K_p occurrence for F10.7 $\le$ 100 (solid line), 100 < F10.7 < 170 (dashed line), and F10.7 $\ge$ 170 (dotted line).

The bottom panel of Fig. 5 shows that there are fewer F1-layers at solar maximum; the middle panel of Fig. 5 shows that there are more occasions when the F1-layer is stronger than the F2-layer at solar maximum. The value of Ψ_G(F10.7) is increased from 0.17% to 0.49% when the F10.7 index increases from F10.7 = 144–170 to F10.7 = 248–274. The latter occurrence must be due to an increase in occasions at solar maximum when the F2 peak density is depressed below the F1 peak density.

The middle and bottom panels of Fig. 6 show that at high solar activity, the F10.7 trend in the probability of strong and very strong $NmF2$ negative disturbances has the higher influence on Ψ_G(F10.7) compared with the F10.7 trend in the F1-layer occurrence probability. However, the F10.7 trend in the probability of strong and very strong $NmF2$ negative disturbances can result from a possible relationship between K_p and F10.7 indices and the K_p trend in the probability of $NmF2$ negative disturbances shown in Fig. 3. To investigate this relationship between K_p and F10.7 indices for the studied time period, we divide the F10.7 range into three intervals F10.7 $\le$ 100, 100 < F10.7 < 170, and F10.7 $\ge$ 170, which correspond approximately to low, moderate, and high solar activity, respectively. We then estimate conditional probabilities, $\Psi_{F10.7\le100}(K_p)$, $\Psi_{100<F10.7<170}(K_p)$, and $\Psi_{F10.7\ge170}(K_p)$ for different values of K_p to occur, pro-

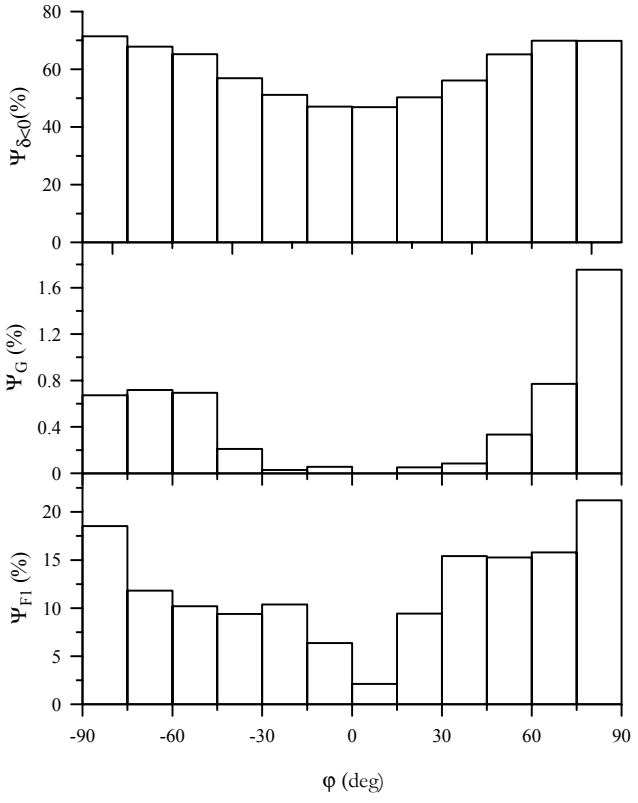

Fig. 8. The dependence of the F1-layer (bottom panel), G condition (middle panel) and NmF2 negative disturbance (top panel) probability functions on the geomagnetic latitude.

vided the index F10.7 is within the intervals specified by the subscripts. The calculated values of $\Psi_{\mathrm{F10.7}\leq 100}(K_p)$, $\Psi_{100<\mathrm{F10.7}<170}(K_p)$ and $\Psi_{\mathrm{F10.7}\geq 170}(K_p)$ are shown in Fig. 7 by solid, dashed, and dotted lines, respectively. It can be seen from Fig. 7 that the conditional probability for low values of K_p (approximately below $2_0\ -2_+$) to occur is decreased as the solar activity increases while the high values of K_p (approximately above $2_+\ -3_0$) become more probable. These results are in agreement with the well-known fact that magnetic storms are more frequent on average at solar maximum than at solar minimum (Field et al., 1998). Thus, at least in part, the F10.7 trends in the probabilities of strong and very strong NmF2 negative disturbances can arise from the K_p trends in the probabilities of these NmF2 negative disturbances shown in Fig. 3.

The middle panel of Fig. 5 shows that the G condition probability has oscillations above F10.7 = 274 that can be explained by oscillations in $\Psi_{\delta\leq -0.3}$(F10.7) and $\Psi_{\delta\leq -0.5}$(F10.7). We did not find any physical explanation of these oscillations in $\Psi_{\delta\leq -0.3}$(F10.7) and $\Psi_{\delta\leq -0.5}$(F10.7); further work is required to express this result in physical processes that determine the value of $fof2$.

4.3 Geomagnetic latitude variations in the F1-layer, G condition and NmF2 negative disturbance occurrence probabilities

Figure 8 displays the histograms of the dependence of the F1-layer (bottom panel), the G condition (middle panel) and NmF2 negative disturbance (top panel) percentage occurrence on the geomagnetic latitude for the Northern ($\varphi > 90°$) and Southern ($\varphi < 90°$) Hemispheres separately. The first thing to note is that the F1-layer occurrence probability has a minimum value of 2.1–6.4% in the magnetic latitude range from –15° to 15°, close to the magnetic equator. The value of $\Psi_{\mathrm{F1}(\varphi)}$ reaches 15.4–15.8% at the magnetic latitudes 30–75° in the Northern Hemisphere and 9.4–11.8% in the magnetic latitude range from -30 to $-75°$ in the Southern Hemisphere. We found the Northern Hemisphere $\Psi_{\mathrm{F1}(\varphi)}$ peak value of 8.5% at the magnetic latitudes 75–90° and the Southern Hemisphere $\Psi_{\mathrm{F1}(\varphi)}$ peak value of 21.2% in the magnetic latitude range from $-75°$ to $-90°$. It is necessary to point out that the trend in $\Psi_{\mathrm{F1}(\varphi)}$ is in agreement with the previous F1-layer studies (Cummack, 1961; Polyakov et al., 1968; Ratcliffe, 1972) based on a more limited data set. At the same time, as far as the authors know, we found for the first time that the magnetic latitude variation of the F1-layer occurrence probability is asymmetrical relative to the geomagnetic equator.

The probabilities $\Psi_{\delta\leq -0.1}(\varphi)$, $\Psi_{\delta\leq -0.3}(\varphi)$, and $\Psi_{\delta\leq -0.5}(\varphi)$ of the NmF2 negative disturbance occurrence are shown in the top, middle, and bottom panels of Fig. 9, respectively. The top panels of Fig. 8 and 9 show that the NmF2 negative disturbance occurrence probabilities $\Psi_{\delta<0}(\varphi)$ and $\Psi_{\delta\leq -0.1}(\varphi)$ have minimum values of 46.9–47.0% and 19.8–21.6%, respectively, in the same low latitude range from $-15°$to 15° and their dependence on the geomagnetic latitude is approximately symmetric with respect to the magnetic equator. Our results clearly show the latitude dependence of $\Psi_{\delta\leq\delta 0}(\varphi)$, reproducing the tendency for decreased $\Psi_{\delta\leq\delta 0}(\varphi)$ at low latitudes and increased $\Psi_{\delta\leq\delta 0}(\varphi)$ at high latitudes.

The middle panel of Fig. 8 shows an interhemispheric asymmetry, calculated for the G condition occurrence probability in the ionosphere, with a stronger enhancement seen in the magnetic latitude range of 75–90° close to the northern magnetic pole. We see a sharp increase in $\Psi_{\mathrm{G}}(\varphi)$ in the Northern Hemisphere as one goes from middle to high latitudes with $\Psi_{\mathrm{G}}(\varphi) = 1.75\%$ at magnetic latitudes 75–90° whereas we compute $\Psi_{\mathrm{G}}(\varphi) = 0.67$–$0.72\%$ from $-45°$ to $-90°$ in the Southern Hemisphere. We can also see a deep minimum of the G condition occurrence probability in the low magnetic latitude range from $-30°$ to 30°. Comparison of $\Psi_{\mathrm{G}}(\varphi)$ and Ψ_{F1} shows that the G condition pattern is more symmetrical about the geomagnetic equator than the F1-layer pattern.

This G condition occurrence probability variation is caused by the F1-layer occurrence probability variation and the geomagnetic latitude trend in $\Psi_{\delta<0}(\varphi)$ shown in the bottom and top panels of Fig. 8, respectively. The fact that the

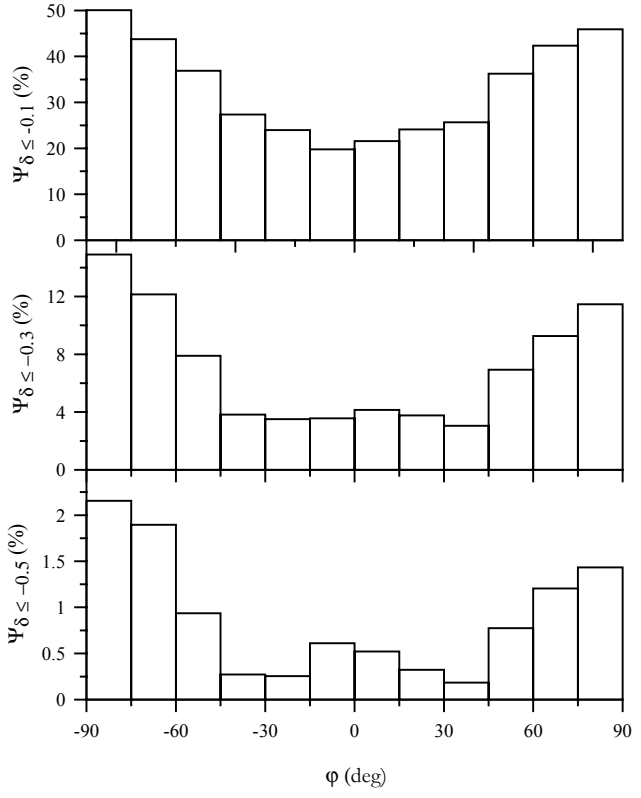

Fig. 9. The dependence of the NmF2 negative disturbance probability functions on the geomagnetic latitude for the values of the NmF2 negative disturbance amplitude $\delta \le -0.1$ (top panel), $\delta \le -0.3$ (middle panel) and $\delta \le -0.5$ (bottom panel).

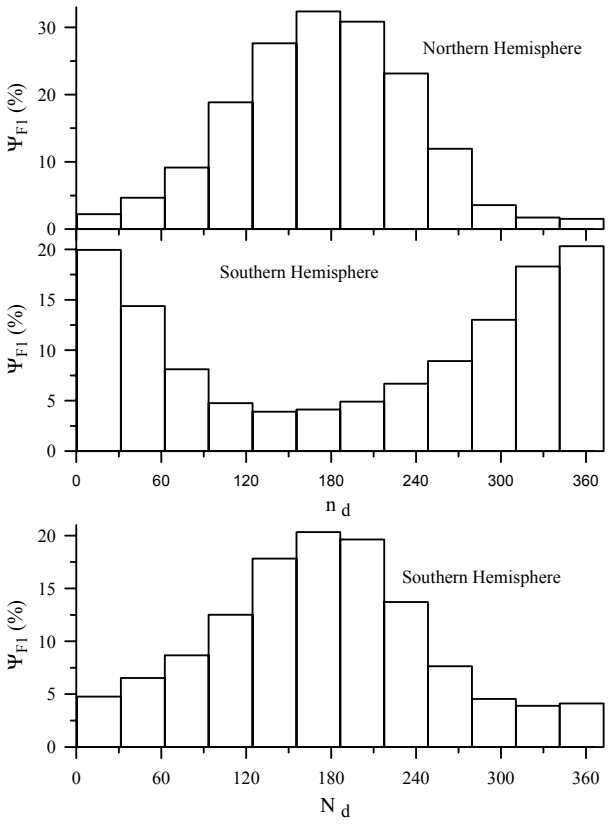

Fig. 10. The dependence of the F1-layer probability function on a number, n_d, of a given day of year for the Northern (top panel) and Southern (middle panel) Hemispheres. The seasonal components of each hemisphere are about 6 months out of phase. As a result, to compare the F1-layer probability function seasonal effects in the Northern (top panel) and Southern (middle panel) Hemispheres we compare the dependence of the F1-layer probability function on N_d in both hemispheres, where the value of N_d is calculated as $N_d = n_d + 183$ for $0 \le n_d \le 183$ and $N_d = n_d - 183$ for $n_d > 183$ in the Southern Hemisphere. The bottom panel shows the resulting dependence of the F1-layer probability function on N_d for the Southern Hemisphere. In the Northern Hemisphere, the value of N_d is the same as n_d, i.e. $\Psi_{F1}(N_d) = \Psi_{F1}(n_d)$.

G condition occurrence is more probable at middle and high magnetic latitudes than at low magnetic latitudes is in agreement with a similar feature of the F1-layer occurrence, and the fact that geomagnetic storm reduction in NmF2, with respect to estimated quiet-time values, is greatest at high geomagnetic latitudes as shown in Fig. 9 and the top panel of Fig. 8 and discussed in previous studies by Zevakina and Kiseleva (1985), Wrenn et al. (1987), and Brunelli and Namgaladze (1988). As the F1-layer occurrence probability variation is asymmetrical, relative to the geomagnetic equator, it appears reasonable to assume that the G condition occurrence probability interhemispheric asymmetry can be due to the $\Psi_{F1}(\varphi)$ asymmetry found in this paper.

4.4 Seasonal variations in the F1-layer and G condition occurrence probabilities

Figures 10 and 11 show histograms of the seasonal dependence of the F1-layer and G condition percentage occurrence for the Northern (top panels) and Southern (middle and bottom panels) Hemispheres, respectively, where n_d is the number of a given day in a year. Comparison of the top and middle panels of Figs. 10 and 11 shows that the seasonal components of each hemisphere are about 6 months out of phase. To show this more easily we introduce a new parameter, N_d. In the Southern Hemisphere, the value of N_d is calculated as $N_d = n_d + 183$ for $0 \le n_d \le 183$ and $N_d = n_d - 183$ for $n_d > 183$. In the Northern Hemisphere, the value of N_d is the same as n_d.

Comparison of the top and bottom panels of Fig. 10 shows that the F1-layer occurrence probability has a maximum value of 32.4 and 20.3% in the Northern and Southern Hemisphere, respectively, which occurs in summer in the N_d range from 152 to 183. The maximum reduction in Ψ_{F1} occurs in winter when the F1-layer occurrence probability reaches the minimum value of 1.5 and 3.9% in the Northern and Southern Hemisphere, respectively.

We can sum the observations in both hemispheres for the same values of N_d. The resulting seasonal dependence of the occurrence of the G condition (top panel) and F1-layer (bot-

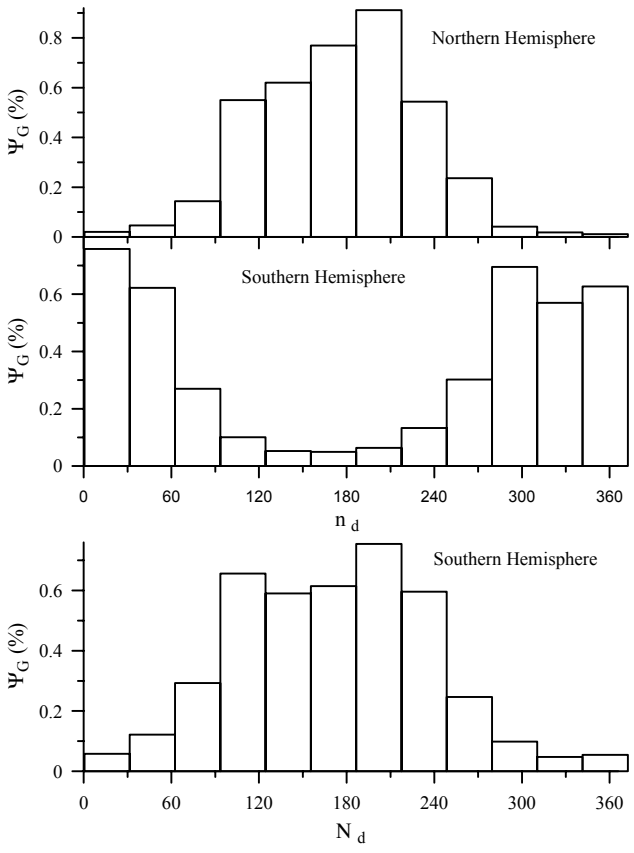

Fig. 11. The dependence of the G condition probability function on a number, n_d , of a given day in a year for the Northern (top panel) and Southern (middle panel) Hemispheres. The seasonal components of each hemisphere are about 6 months out of phase. As a result, to compare the G condition probability function seasonal effects in the Northern (top panel) and Southern (middle panel) Hemispheres we compare the dependence of the G condition probability function on N_d in both hemispheres, where the value of N_d is calculated as $N_d = n_d + 183$ for $0 \leq n_d \leq 183$ and $N_d = n_d - 183$ for $n_d > 183$ in the Southern Hemisphere. The bottom panel shows the found dependence of the G condition probability function on N_d for the Southern Hemisphere. In the Northern Hemisphere, the value of N_d is the same as n_d, i.e. $\Psi_G(N_d) = \Psi_G(n_d)$.

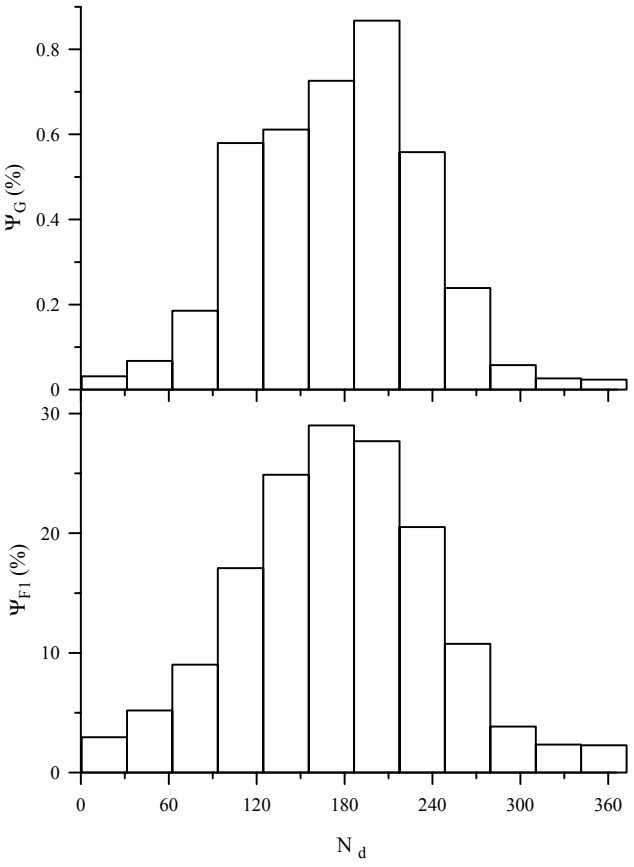

Fig. 12. The seasonal dependence of the F1-layer (bottom panel), and G condition (top panel) probability functions in both hemispheres.

tom panel) probability on N_d in both hemispheres is shown in Fig. 12. It can be seen from the bottom panel of Fig. 12 that the F1-layer occurrence probability reaches a maximum value of 29.0% in the N_d range from 152 to 183.

In previous F1-layer studies (Polyakov et al., 1968; Ratcliffe, 1972; Shchepkin et al., 1984), based on a limited data set, it was demonstrated that the chance that the F1-layer will be formed is greater in summer than in winter; our results provide additional evidence of this phenomenon, giving a more detailed picture of the F1-layer seasonal behaviour. At the same time, as far as the authors know, we found for the first time that the Northern Hemisphere peak F1-layer occurrence probability shown in the top panel of Fig. 10 exceeds the Southern Hemisphere peak F1-layer occurrence probability shown in the bottom panel of Fig. 10.

We now examine the G condition occurrence probability shown in Fig. 11 and find a Ψ_G (N_d) maximum value of 0.91 (top panel of Fig. 11) and 0.75% (bottom panel of Fig. 11) in the Northern and Southern Hemispheres, respectively; this occurs in summer in the N_d range from 183 to 213. The value of $\Psi_G(N_d)$ reaches its hemisphere minimum value of 0.01 (top panel of Fig. 11) and 0.05% (bottom panel of Fig. 11) in winter in the Northern and Southern Hemisphere, respectively.

Figure 12 presents the calculated values of Ψ_{F1} (N_d) (bottom panel) and $\Psi_G(N_d)$ (top panel) that take into account the seasonal variations of the F1-layer and G condition occurrence probabilities in both hemispheres. One can see that this averaging leads to the G condition occurrence probability maximum value of 0.87% in summer in the N_d range from 183 to 213. The minimum of $\Psi_G(N_d)$ is located in winter in the N_d interval 332–366.

Ionosonde fof2 measurements from the Argentine Islands ionozonde station for 1971–1981 were analyzed by Wrenn et al. (1987). Wrenn et al. (1987) distinguished geomagnetic activity levels as very quiet, quiet, normal, disturbed and very disturbed conditions; they found that the large negative ionospheric storm effect in NmF2 during very geomagnetically disturbed conditions, is usually observed in summer. The

dominance of $NmF2$ negative storm effects in summer compared to winter was shown by Putz et al. (1990) for three European stations. At Stanford, USA, in summer, the negative effects were much larger than the positive ones (Titheridge and Buonsanto, 1988) and, in winter, positive effects dominate (Putz et al., 1990; Titheridge and Buonsanto, 1988). A decrease in the [O]/[N_2] and [O]/[O_2] thermospheric ratios at high and middle latitudes during geomagnetic storms has been suggested as the cause of the negative phase for many years; this has been demonstrated clearly with satellite data (Prolss, 1995). As is well known (for more details see Sect. 4.1), this ratio decrease is caused by magnetic storm equatorward winds from high latitudes to the geomagnetic equator; this mechanism is especially effective in the summer hemisphere where the quiet mid-latitude circulation is already equatorward (Fuller-Rowell et al., 1996). The boundary between N_2 and O_2 geomagnetic storm enrichment and N_2 and O_2 geomagnetic storm depletion is sharper and lies at higher latitude in winter as compared with summer (Prolss, 1995; Richmond and Lu, 2000).

During daytime, $NmF2$ is approximately proportional to [O]/L and the [O]/[N_2] and [O]/[O_2] ratio decreases determine decreases in $NmF2$. As a result, the seasonal behaviour of the G condition occurrence probability is found to be related to the seasonal behaviour of the F1-layer and the $NmF2$ negative disturbance occurrence probability.

5 Conclusions

The primary goal of the present work is to find the statistical relationships of the G condition occurrence probability with geomagnetic and solar activity indices K_p and F10.7, season and geomagnetic latitude, using experimental data acquired by the Ionospheric Digital Database of the National Geophysical Data Center, Boulder, Colorado, from 1957 to 1990. The F1-layer is included in our analysis because the G condition cannot exist in the ionosphere if there is no the F1-layer. During ionospheric disturbances, the $NmF2$ decrease leads to an increase in the G condition occurrence probability if the F1-layer exist, and, as a result, relationships exist between the G condition and $NmF2$ negative disturbance occurrence probabilities; these are studied in this paper.

The total probabilities of the G condition and F1-layer occurrences for the time period from 1957 to 1990 were found to be 0.34% and 13.20%, respectively. The total number of hourly $foF2$ disturbance measurements analyzed includes 60% of negative $foF2$ disturbances and 40% of positive $foF2$ disturbances. The analyzed hourly negative $foF2$ disturbances include 47% weak negative $foF2$ disturbances ($-0.1 < \delta < 0$ or $0.81 < NmF2(d)/NmF2(q) < 1$), 43% of normal negative $foF2$ disturbances ($-0.3 < \delta - 0.1$ or $0.49 < NmF2(d)/NmF2(q) \leq 0.81$), 9% of strong negative $foF2$ disturbances ($-0.5 < \delta \leq -0.3$ or $0.25 < NmF2(d)/NmF2(q) \leq 0.49$) and 1% of very strong hourly negative $foF2$ disturbances ($\delta \leq -0.5$ or $NmF2(d)/NmF2(q) \leq 0.25$).

We found that the G condition occurrence probability reveals a strong increase with the increase of K_p whereas variations in the F1-layer occurrence probability do not show significant changes with the K_p variations. It is shown that the dependence of the G condition occurrence probability on K_p is mainly determined by processes that control the behaviour of the F2-layer with K_p changes. The relationship for log $\Psi_G(K_p)$ versus K_p fit well to a straight line. We found that increase of the minimum absolute value of the $NmF2$ negative disturbance amplitude leads to a decrease in the maximum and minimum values of the $NmF2$ negative disturbance occurrence probability and to an increase in the ratio of the maximum value of this probability to its minimum value, i.e. the $NmF2$ negative disturbance occurrence probability dependence shows the stronger positive K_p tendency with the increase in the maximum absolute value of the $NmF2$ negative disturbance amplitude.

The decrease in the probability of observing the F1-layer occurs with the change from solar minimum to solar maximum. As far as the authors know, we found for the first time a positive tendency in the $NmF2$ negative disturbance occurrence probability dependencies on F10.7 for strong and very strong negative $NmF2$ disturbances, while the weak and normal $NmF2$ negative disturbances do not show any dependence of their occurrence probabilities on F10.7. The very interesting feature of the G condition is that the G condition occurrence probability is decreased as the value of F10.7 increases from low to middle values, reaches its minimum at the middle solar activity level of F10.7 = 144–170, followed by an increase when the F10.7 index increases from the middle solar activity level to F10.7 = 248–274. The dependence of the G condition occurrence probability on F10.7 contains contributions from two sources, the F1 and F2-layers. The main source that contributes to the dependence of the G condition occurrence probability on F10.7, at low solar activity, is the dependence of the F1-layer occurrence probability on F10.7, while at high solar activity, the dependence of the $NmF2$ negative disturbance occurrence probability on F10.7 for strong and very strong negative $NmF2$ disturbances is found to be more efficient in maintaining the G condition against the F1-layer F10.7 trend that tends to decrease the G condition occurrence probability. We found that, at least in part, the F10.7 trends in the probabilities of strong and very strong $NmF2$ negative disturbances can arise from the K_p trends in the probabilities of these $NmF2$ negative disturbances.

Our results clearly show latitude dependence in the weak, normal, strong and very strong $NmF2$ negative disturbance occurrence probabilities, reproducing the tendency for decreased probabilities at low latitudes and increased probabilities at high latitudes. It is found that the F1-layer occurrence probability has a minimum value of 2.1–6.4% in the magnetic latitude range from $-15°$ to $15°$, close to the magnetic equator. The value of the F1-layer occurrence probability reaches 15.4–15.8% at magnetic latitudes 30–75° in the Northern Hemisphere and 9.4–11.8% in the magnetic latitude range from -30 to $-75°$ in the Southern Hemisphere.

The magnetic latitude trend in the F1-layer occurrence probability is found to be in agreement with previous F1-layer studies (Cummack, 1961; Polyakov et al., 1968; Ratcliffe, 1972) based on a more limited data set. However, as far as the authors know, we found for the first time that the F1-layer occurrence probability has asymmetrical variation relative to the geomagnetic equator.

Our calculations show an increase in the G condition occurrence probability in the both hemispheres as one goes from middle to high latitudes and a deep minimum of the G condition occurrence probability in the low magnetic latitude range from $-30°$ to $30°$. Interhemispheric asymmetry is found for the G condition occurrence probability in the ionosphere, with stronger enhancement in the magnetic latitude range close to the Northern magnetic pole.

In agreement with the previous F1-layer studies (Polyakov et al., 1968; Ratcliffe, 1972; Shchepkin et al., 1984) based on a limited data set, our results provide additional evidence that the probability that the F1-layer will be formed is greater in summer than in winter. However, as far as the authors know, we found for the first time that the Northern Hemisphere peak F1-layer occurrence probability exceeds that in the Southern Hemisphere.

We found that the G condition occurrence probability maximum value of 0.91 and 0.75% in the Northern and Southern Hemispheres, respectively, occurs in summer. It is shown that the G condition occurrence probability reaches its hemisphere minimum value of 0.01 and 0.05% in winter in the Northern and Southern Hemisphere, respectively.

Acknowledgements. The research described in this publication was supported by grant 99-05-65231 from the Russian Foundation for Basic Research. The authors would like to thank L. N. Leschenko (IZMIRAN) for the useful elucidation of some details of the ionogram treatment rules. We would like to thank anonymous referees for critical reading of the manuscript as reviewers and for helpful comments.

Topical Editor G. Chanteur thanks Y. Su and another referee for their help in evaluating this paper.

References

Badin, V. I.: Analytical dependencies of the electron density and peak height of the daytime F2-layer on plasma drift velocity and other parameters of the atmosphere, Geomagn. Aeron., (in Russian), 29, 795–798, 1989.

Badin, V. I. and Deminov, M. G.: Plasma drift effect on the F2 region ionospheric structure. Ionospheric forecast, Nauka, Moscow, (in Russian), 79–81, 1982.

Banks, P. M., Schunk, R. W., and Raitt, W. J.: NO^+ and O^+ in the high latitude F-region, Geophys. Res. Lett., 1, 239–242, 1974.

Brunelli, B. E. and Namgaladze, A. A.: Physics of the ionosphere (in Russian), Nauka, Moscow, 1988.

Buonsanto, M. J.,: Observed and calculated F2 peak heights and derived meridional winds at mid-latitudes over a full solar cycle, J. Atmos. Terr. Phys., 52, 223–240, 1990.

Cummack, C. H.: Evidence of some geomagnetic control of the F1-layer, J. Atmosph. Terr. Phys., 22, 157–158, 1961.

Fejer, B. G.: The electrodynamics of the low latitude ionosphere: recent results and future challenges, J. Atmos. Terr. Phys., 59, 1465–1482, 1997.

Field, P. R., Rishbeth, H., Moffett, R. J., Idenden, D. W., Fuller-Rowell, T. G., Millward, G. H., and Aylward, A. D.: Modelling composition changes in F-layer storms, J. Atmosph. Terr. Phys., 60, 523–543, 1998.

Fukao, S., Oliver, W. L., Onishi, Y., Takami, T., Sato, T., Tsuda, T., Yamamoto, M., and Kato, S.: F- region seasonal behaviour as measured by the MU radar, J. Atmos. Terr. Phys., 53, 599–618, 1991.

Fuller-Rowell, T. J., Codrescu, M. V., Moett, R. J., and Quegan S.: On the seasonal response of the thermosphere and ionosphere to geomagnetic storms, J. Geophys. Res., 101, 2343–2353, 1996.

Fuller-Rowell, T. J., Codrescu, M. V., and Wilkinson, P.: Quantitative modeling of the ionospheric response to geomagnetic activity, Ann. Geophysicae, 18, 766–781, 2000.

Häggström, I. and Collis, P. N.: Ion composition changes during F-region density depletions in the presence of electric fields at auroral latitudes, J. Atmos. Terr. Phys., 52, 519–529, 1990.

Hedin, A. E.: MSIS-86 thermospheric model, J. Geophys. Res., 92, 4649–4662, 1987.

Hierl, M. P., Dotan, I., Seeley, J. V., Van Doren, J. M., Morris, R. A., and Viggiano, A. A.: Rate constants for the reactions of O^+ with N_2 and O_2 as a function of temperature (300–1800 K), J. Chem. Phys. 106, 3540–3544, 1997.

King, G. A. M.: The ionospheric F-region during a storm, Planet. Space Sci., 9, 95–100, 1962.

Mednikova, N. V.: Delay of ionospheric storms relative to magnetic storms (in Russian), Ionospheric variations during magnitospheric disturbances, Nauka, Moscow, 120–124, 1980.

Norton, R. B.: The middle-latitude F-region during some severe ionospheric storms, Proc. IEEE, 57, 1147–1149, 1969.

Oliver, W. L.: Neutral and ion composition changes in the F-region over Millstone Hill during the equinox transition study, J. Geophys. Res., 95, 4129–4134, 1990.

Pavlov, A. V.: The role of vibrationally excited nitrogen in the ionosphere, Pure Appl. Geophys., 127, 529–544, 1988.

Pavlov, A. V.: The role of vibrationally excited nitrogen in the formation of the mid-latitude ionospheric storms, Ann. Geophysicae, 12, 554–564, 1994.

Pavlov, A. V.: Subauroral red arcs as a conjugate phenomenon: comparison of OV1-10 satellite data with numerical calculations, Ann. Geophysicae, 15, 984–998, 1997.

Pavlov, A. V.: The role of vibrationally excited oxygen and nitrogen in the ionosphere during the undisturbed and geomagnetic storm period of 6–12 April 1990, Ann. Geophysicae, 16, 589–601, 1998.

Pavlov, A. V. and Buonsanto, M. J.: Comparison of model electron densities and temperatures with Millstone Hill observations during undisturbed periods and the geomagnetic storms of March 16–23 and April 6–12, 1990, Ann. Geophysicae, 15, 327–344, 1997.

Pavlov, A. V. and Buonsanto, M. J.: Anomalous electron density events in the quiet summer ionosphere at solar minimum over Millstone Hill, Ann. Geophysicae, 16, 460–469, 1998.

Pavlov, A. V., Buonsanto, M. J., Schlesier, A. C., and Richards, P. G.: Comparison of models and data at Millstone Hill during the 5–11 June, 1991, storm, J. Atmosph. Terr. Phys., 61, 263–279, 1999.

Pavlov, A. V. and Namgaladze, A. A.: Vibrationally excited molecular nitrogen in the upper atmosphere, (Review), Geomagn.

Aeron., 28, 607–619, 1988.

Pavlov, A. V. and Oyama, K.-I.: The role of vibrationally excited nitrogen and oxygen in the ionosphere over Millstone Hill during 16–23 March 1990, Ann. Geophysicae, 18, 957–966, 2000.

Pavlov, A. V., Abe, T., and Oyama, K.-I.: Comparison of the measured and modelled electron densities and temperatures in the ionosphere and plasmasphere during 20–30 January 1993, Ann. Geophysicae, 18, 1257–1272, 2000.

Pavlov, A. V., Abe, T., and Oyama, K.-I.: Comparison of the measured and modeled electron densities and temperatures in the ionosphere and plasmasphere during the period of 25–29 June 1990, J. Atmosph. Terr. Phys., 63, 605–616, 2001.

Polyakov, I. A., Shchepkin, L. A., Kazimirovsky, E. S. and Kokourov, V. D.: Ionospheric processes (in Russian), Nauka, Novosibirsk, 1968.

Prolss, G. W.: Magnetic storm associated perturbations of the upper atmosphere: Recent results obtained by satellite-borne gas analyzers, Rev. Geophys. Space Phys., 18, 183–202, 1980.

Prolss, G. W.: Ionospheric F-region storms, in: Handbook of Atmospheric Electrodynamic, (Ed) Volland, H., Vol. 2, P. 195–248. CRC Press, Boca Raton, FL, 1995.

Putz, E., Jakowski, N., and Spalla, P.: Statistische Untersuchungen von Ionosphärenstürmen und erste Modellrechnungen, Klein-Heubacher Ber., 33, 121–129, 1990.

Radzig, A. A. and Smirnov, B. V.: Reference data on atoms, molecules and ions, Springer Verlag, Berlin, 1985.

Ratcliffe, J. A.: An introduction to the ionosphere and magnetosphere, Cambridge, University Press, 1972.

Rees, M. H.: Physics and chemistry of the upper atmosphere, Cambridge and New York, Cambridge University Press, 1989.

Richards, P. G., Fennelly, J. A., and Torr, D. G.: EUVAC: A solar EUV flux model for aeronomical calculations, J. Geophys. Res., 99, 8981–8992, 1994, Correction in J. Geophys. Res., 99, 13 283, 1994.

Richmond, A. D. and Lu, G.: Upper-atmospheric effects of magnetic storms: a brief tutorial, J. Atmosph. Terr. Phys., 62, 1115–1127, 2000.

Rishbeth, H. and Garriot, O.: Introduction to ionospheric physics, New York, Academic Press, 1969.

Rishbeth, H. and Muller-Wodarg, I. C. F.: Vertical circulation and thermospheric composition: a modelling study, Ann. Geophysicae, 17, 794–805, 1999.

Rishbeth, H., Muller-Wodarg, I. C. F., Zou, L., Fuller-Rowell, T. J., Millward, G. H., Moffett, R. J., D. W. Idenden, and Aylward, A. D.: Annual and semiannual variations in the ionospheric F2-layer: II. Physical discussion, Ann. Geophysicae, 18, 945–956, 2000.

Strobel, D. F. and McElroy, M. B.: The F2-layer at middle latitudes, Planet. Space Sci., 18, 1181–1202, 1970.

Schlesier, A. C. and Buonsanto, M. J.: Observations and modeling of the 10–12 April 1997 ionospheric storm at Millstone Hill, Geophys. Res. Lett., 26, 2359–2362, 1999.

Schmeltekopf, A. L., Ferguson, E. E., and Fehsenfeld, F. C.: Afterglow studies of the reactions He^+, $He(^2S)$, and O^+ with vibrationally excited N_2, J. chem. Phys, 48, 2966–2973, 1968.

Schunk, R. W., Raitt, W. J., and Banks, P. M.: Effects of electric fields on the daytime high-latitude E and F-regions, J. Geophys. Res., 80, 3121–3130, 1975.

Shchepkin, L. A., Vasiliev, K. N., Vinitskii, A. V., Grishkevich, L. V., Datsko, E. P., Kushnarenko, G. P., Moskaliuk, N. V., and Shulgina, V. I.: Seasonal variations of F1-layer parameters in a solar-maximum period (in Russian), Geomagnetism and Aeronomy, 34, 35–39, 1984.

St.-Maurice, J.-P. and Torr, D. G.: Nonthermal rate coefficients in the ionosphere: The reactions of O^+ with N_2, O_2 and NO, J. Geophys. Res., 83, 969–977, 1978.

Torr, M. R., Torr, D. G., Richards, P. G., and Yung, S. P.: Mid- and low-latitude model of thermospheric emissions. 1. $O^+(^2P)$ 7320 A and $N_2(^2P)$ 3371 A, J. Geophys. Res., 95, 21 147–21 168, 1990.

Titheridge, J. E. and Buonsanto, M. J.: A comparison of Northern and Southern hemisphere TEC storm behaviour, J. Atmos. Terr. Phys., 50, 763–780, 1988.

URSI handbook of ionogram interpretation and reduction, (Eds) Piggott, W. R. and Rawer, K., National Oceanic and Atmospheric Administration, Boulder, CO, 1978.

Wrenn, G. L., Rodger, A. S., and Rishbeth, H.: Geomagnetic storms in antarctic F-region. I. Diurnal and seasonal patterns for main phase effects, J. Atmosph. Terr. Phys., 49, 901–913, 1987.

Zevakina, R. A. and Kiseleva, M. V.: About the quantitative forecast possibility of negative ionospheric disturbances (in Russian), Forecasting applied to the ionosphere and conditions of radiowave propagation, Nauka, Moscow, 39–43, 1985.

Zuzic, M., Scherliess, L. and Prolss, G. W.: Latitudinal structure of thermospheric composition perturbations, J. Atmosph. Terr. Phys., 59, 711–724, 1997.